

D. A. DaDeppo

Professor,

Department of Civil Engineering
and Engineering Mechanics,
The University of Arizona,
Tucson, Ariz. Mem. ASME

R. Schmidt

Professor of Engineering Mechanics,
Department of Civil Engineering,
University of Detroit,
Detroit, Mich. Mem. ASME

Large Deflections and Stability of Hingeless Circular Arches Under Interacting Loads

The buckling behavior subsequent to large prebuckling deflections of hingeless circular arches subjected to a downward point load at the crown as well as their own dead weight is investigated on the basis of Euler's nonlinear theory of the inextensible curved elastica. The theory used is exact in the sense that no restrictions are imposed on the magnitudes of deflections. Among others, interaction curves of the critical values of the two loads (i.e., stability boundaries) are plotted and examined. With the aid of these interaction curves, simple approximate formulas relating the two critical loads are established. It is found that nonshallow hingeless arches may buckle by either asymmetrical sidesway or symmetrical snap-through, depending on the relative magnitudes of the point load and the weight of the arch. The results of this study are essential if arches are to be tested near buckling loads, since it is difficult to eliminate the effect of own dead weight in experimental work.

Introduction

The classical theory of stability of arches is concerned with the calculation of the critical value of the load on a nonshallow arch whose shape is coincident (or nearly such) with the pressure line of the loads. In these cases the prebuckling deflections are small. In other cases of load, the instability of slender arches is preceded by large deflections which considerably complicate the (nonlinear) analysis. Nevertheless, several problems of buckling and postbuckling behavior of arches with preceding large deflections have been solved accurately for different types of load with the aid of digital computers.

In [1]¹ Huddleston calculated, by means of a numerical technique, the critical value of a downward point load at the crown, corresponding to the first bifurcation point in the load-deflection diagram, for a two-hinged circular arch with a height-to-span ratio of 0.25. The buckling mode was asymmetrical, a sidesway mode. The theories of the inextensible and extensible elastica were used in separate analyses of the same arch. However, for

nonshallow slender arches buckling at large deflections, the inextensible theory yields sufficiently accurate results for all practical purposes. The critical loads for circular arches with different subtending angles 2α were calculated in [2, 5] on the basis of the inextensible theory employing elliptic integrals. Several approximate analyses are extant, too [11, 12].

The instability of hingeless circular arches under a downward point load P at the crown has also been investigated recently [7]. While the nonshallow two-hinged arch under this type of load buckles asymmetrically by sidesway, the hingeless arch buckles symmetrically by snap-through for $\alpha < \alpha^* \approx 135$ deg and by sidesway for $\alpha > \alpha^*$. Large deflections of hingeless circular arches subjected to a point load P were analyzed by Nordgren [8] with the assumption of symmetric deflections. This assumption made the decision concerning the value of the actual buckling load impossible. Nordgren obtained a typical snap-through plot of P versus v_c for $\alpha = 45$ deg. The relative maximum occurred at $P = 19.3EI/a^2$, where a is the radius of the undeformed arch, a value which coincides with that obtained in [7]. Two experiments [8] yielded $Pa^2/EI = 18.5$ and 17.9 , i.e., 4.1 and 7.3 percent less than the calculated value. These discrepancies are likely to be due at least in part to the effect of the own weight of the specimen.

The problem of the critical value of the own weight of unloaded circular arches was investigated in [6, 9]. For example, the critical values of the total weight $W_{cr} = 7.85EI/a^2$ and $25.9EI/a^2$ of the two-hinged and hingeless semicircular arches are considerably higher than the critical values of the point load $P_{cr} = 5.86EI/a^2$ and $10.45EI/a^2$, respectively. Both the two-hinged and hingeless high-rise arches under their own weight buckle by sidesway.

¹ Numbers in brackets designate References at end of paper.

Presented at the Seventh U. S. National Congress of Applied Mechanics, University of Colorado, Boulder, Colo., June 3-7, 1974.

Discussion on this paper should be addressed to the Editorial Department, ASME, United Engineering Center, 345 East 47th Street, New York, N. Y. 10017, and will be accepted until February 15, 1975. Discussion received after this date will be returned. Manuscript received by ASME Applied Mechanics Division, December, 1973; final revision, April, 1974.

As indicated in the following paragraph, the effect of the interaction of the dead weight and applied load on the stability of an arch is of considerable interest in experimental work, since it is very difficult to eliminate the dead weight of the specimen. Calculations seem to offer the best means of determining the percentage to be added to the measured critical load acting on the arch in order to arrive at, or near, the value of the load predicted by theory.

Langhaar, Boresi, and Carver [3] calculated an approximate critical value of the vertical point load P applied at the crown of the two-hinged semicircular arch. An experimental verification of the calculated value required a correction due to the own weight of the test specimen. It was assumed, on the basis of Euler's theory of buckling of columns, that the total weight of the arch may be lumped together with the concentrated load applied at the crown. Lind [4], after some comparative experimentation with arches prestressed in flexure, arrived at the tentative conclusion that only one half to two thirds of the total weight should be used in the modification of the critical point load. A more exact analysis has yielded the following approximate (but very accurate) relation between the critical values of the applied load and the arch's own weight [13]:

$$P = \left(1 - \frac{w}{w_{cr}}\right) P_{cr}$$

in which the values of P_{cr} and w_{cr} can be taken from [2, 5, 9], respectively. Unfortunately, no such simple relation can be written for very heavy arches with clamped ends.

A more extensive survey of literature on large deflections and stability of nonshallow arches can be found in [14].

The present study is concerned with the relatively difficult and laborious problem of determining relations between the critical values of the applied point load and the own weight of hingeless circular arches of uniform cross section. Such nonshallow arches buckle in a symmetric mode (snap-through), if light, and in an asymmetric mode (sidesway), if heavy. The nonlinear boundary-value problem of the inextensible elastica is solved numerically to a high degree of accuracy, which is ascertained by comparisons with some known exact solutions of related problems [2, 5]. Stability boundaries (i.e., critical load interaction diagrams), critical deflections, prebuckling and buckling configurations, and moment and thrust diagrams are established for different values of the subtending angle of the arch.

Governing Equations

According to [10], the extensional strain ϵ of the centroidal curve of the arch rib is given by the equation

$$2\epsilon + \epsilon^2 = 2e + e^2 + \omega^2 \quad (1)$$

where

$$e = \kappa(u' \cos \phi + v' \sin \phi) = (1 + \epsilon) \cos \beta - 1 \quad (2a)$$

$$\omega = \kappa(-u' \sin \phi + v' \cos \phi) = (1 + \epsilon) \sin \beta \quad (2b)$$

κ is the radius of curvature of the undeformed centroidal curve, u and v are the horizontal and vertical (downward) displacement components of a point on the centroidal curve, and prime denotes derivative with respect to the angle ϕ formed by a normal to the undeformed centroidal curve and a vertical reference line, i.e., $u' = du/d\phi$. The change of curvature $\kappa^* - \kappa$ is given by

$$\kappa^* - \kappa = \frac{\kappa(\beta' - \epsilon)}{1 + \epsilon} \quad (3)$$

where κ^* is the curvature of the deformed centroidal curve and β the angle of rotation of a tangent,

$$\beta = \arcsin \frac{\omega}{1 + \epsilon} = \arccos \frac{1 + \epsilon}{1 + \epsilon} = \arctan \frac{\omega}{1 + \epsilon} \quad (4)$$

$$\beta' = \frac{(1 + \epsilon)\omega' - \epsilon'\omega}{(1 + \epsilon)^2} \quad (5)$$

The Winkler-Bach hypothesis of rigid normal cross sections and Hooke's law lead to the following expression for the normal stress σ :

$$\sigma = E \frac{\epsilon - z\kappa\beta'}{1 - \kappa z} \quad (6)$$

where E is the modulus of elasticity and z the inward normal distance from the centroidal curve.

The strain energy Π_s in the arch rib is given by the usual integral expression

$$\Pi_s = \frac{1}{2E} \iiint \sigma^2 (a - z) d\phi dA \quad (7)$$

which, after substitution of equation (6) with $\epsilon = 0$ (inextensible centroidal line), becomes

$$\Pi_s = \frac{E}{2a} \int_{-\alpha}^{\alpha} J \cdot (\beta')^2 d\phi \quad (8)$$

where

$$J = \iint \frac{z^2 dA}{1 - \kappa z} \quad (9)$$

J being approximately equal to the moment of inertia of the cross-sectional area, I , in the case of slender arch ribs. The potential energy of the two interacting loads is

$$\Pi_l = Pv_c - wa \int_{-\alpha}^{\alpha} vd\phi \quad (10)$$

In order to derive the equation of equilibrium in β or $\theta = \phi + \beta$ for a circular arch, we make use of the principle of stationary potential energy in conjunction with the calculus of variations. In view of the constraining condition $\epsilon = 0$ and equation (1), the functional to be dealt with is

$$F = \int_{-\alpha}^{\alpha} f d\phi - Pv_c = \Pi_s + \Pi_l + \lambda a \int_{-\alpha}^{\alpha} \left[e + \frac{1}{2}(e^2 + \omega^2) \right] d\phi \quad (11)$$

where λ is Lagrange's multiplier and

$$f(\phi; v, u', v', u'', v'') = \frac{EJ}{2a} (\beta')^2 - wav + a\lambda \left[e + \frac{1}{2}(e^2 + \omega^2) \right] \quad (12)$$

Since $\partial f / \partial u = 0$ and $\partial f / \partial v = -wa$, a set of the two Euler equations can be written in the integrated form

$$\frac{\partial f}{\partial u'} - \left(\frac{\partial f}{\partial u''} \right)' = -H, \quad \frac{\partial f}{\partial v'} - \left(\frac{\partial f}{\partial v''} \right)' = -wa\phi + V_0 \quad (13)$$

in which H and V_0 are the constants of integration and

$$\frac{\partial f}{\partial u'} = [\kappa^2 EJ\beta'(\beta' - 1) + \lambda] \cos(\phi + \beta) \quad (14a)$$

$$\frac{\partial f}{\partial v'} = [\kappa^2 EJ\beta'(\beta' - 1) + \lambda] \sin(\phi + \beta) \quad (14b)$$

$$\frac{\partial f}{\partial u''} = -\kappa^2 EJ\beta' \sin(\phi + \beta) \quad (14c)$$

$$\frac{\partial f}{\partial v''} = \kappa^2 EJ\beta' \cos(\phi + \beta) \quad (14d)$$

in view of equations (5) and (2), and the condition of inextension-

ality $\epsilon = 0$. Substituting equations (14) in equations (13) and letting $\theta = \phi + \beta$, we obtain

$$\kappa^2 EJ[\theta'' \sin \theta + 2(\theta' - 1)^2 \cos \theta] + \lambda \cos \theta = -H \quad (15a)$$

$$\begin{aligned} \kappa^2 EJ[-\theta'' \cos \theta + 2(\theta' - 1)^2 \sin \theta] + \lambda \sin \theta \\ = -aw\phi + V_0 \end{aligned} \quad (15b)$$

Multiplying equations (15a) and (15b) by $\sin \theta$ and $\cos \theta$, respectively, and subtracting, we obtain the following governing equation:

$$\kappa^2 EJ\theta'' + H \sin \theta + (V_0 - aw\phi) \cos \theta = 0 \quad (16)$$

Equation (16) must be supplemented by the geometrical relations [2]

$$x' = a \cos \theta, \quad y' = a \sin \theta \quad (17)$$

and the appropriate boundary conditions.

In the case of vanishing own dead weight, $w = 0$, a downward point load acting on the crown, and hinged ends, the foregoing nonlinear boundary-value problem was solved exactly [2, 5] with the aid of elliptic integrals. In the case of nonvanishing w , no exact method of solution is known. For this reason, the problem has been solved numerically with a high degree of accuracy. Since, it is felt, numerical techniques are of little technical interest and their detailed description consumes considerable space, only an outline of the integration procedure employed is presented herein. Motivation for the procedure follows from a consideration of stability of equilibrium.

We note that the critical value of the point load, for a given value W of own weight, is associated with either a limit point (a local maximum) for symmetric buckling or a bifurcation point for asymmetric buckling (sideways) on a plot of the point load P versus vertical displacement v_c of the crown. A test for critical loading is derived from the relationship of rate of loading to rate of displacement for quasi-static motion from a current equilibrium state which is represented by a point on the P versus v_c curve. In the following discussion the load applied at the crown is expanded to include a horizontal point load R and a couple M_c . Let $z_1 = \dot{u}_c$, $z_2 = \dot{v}_c$, $z_3 = \dot{\beta}_c$ where \dot{u}_c and \dot{v}_c are components of the linear rate of displacement, and $\dot{\beta}_c$ is the rate of rotation of the tangent to the centroidal line at the crown (load point); let $\dot{p}_1 = \dot{R}$, $\dot{p}_2 = \dot{P}$ and $\dot{p}_3 = \dot{M}_c$ be components of the corresponding rate of loading with \dot{p}_1 and \dot{p}_2 positive to the right and downward, respectively, and \dot{p}_3 positive in the clockwise sense; and let \dot{w} be the rate of uniform loading per unit of arc length. The rates are linearly related and the relation can be written in the form

$$\sum_{j=1}^3 C_{ij}\dot{z}_j = \dot{p}_i + \dot{w}b_i \quad i = 1, 2, 3 \quad (18)$$

The coefficients b_i and the stiffness coefficients $C_{ij} = C_{ji}$ are properties of the arch in its current equilibrium configuration as represented by the current values of u_c , v_c , β_c , and w ; hence, $C_{ij} = C_{ij}(u_c, v_c, \beta_c, w)$. It is assumed that the C_{ij} are continuous functions of u_c , v_c , β_c , and w . We may relate the stiffness coefficients to the second variation of the potential energy function, for all arch configurations satisfying equations (16) and (17) and the boundary conditions, expressed in terms of u_c , v_c , β_c , and w . As the arch passes through a succession of equilibrium states, starting from a stable state and terminating in an unstable equilib-

um state, the quadratic form $\sum_{i,j=1}^3 C_{ij}\dot{z}_i\dot{z}_j$, which is initially posi-

tive-definite, becomes positive-semidefinite and, finally, indefinite. At the critical load the quadratic form becomes positive semidefinite for the first time. The determinant $|C_{ij}|$ and its principal minors characterize the transition from a stable state of equilibrium to a critical state. In the stable state $|C_{ij}|$ and all of its principal minors are positive. As the critical state is approached the determinant tends to zero and all of its principal

minors are nonnegative. Thus $|C_{ij}| = 0$ is the test for critical loading. Now assume that the rate of loading is prescribed in the form $\dot{p}_i = \dot{p}\alpha_i$, $\dot{w} = 0$, where the α_i are constants, so that equation (18) becomes

$$\sum_{j=1}^3 C_{ij}\dot{z}_j = \dot{p}\alpha_i \quad i = 1, 2, 3 \quad (19)$$

The solution values \dot{p} , \dot{z}_i of equations (19), with nontrivial \dot{z}_i , at the critical load determine the character of the critical point. At a limit point equations (19) can be satisfied only if $\dot{p} = 0$.² At a bifurcation point the equations have one solution with $\dot{p} = 0$ and one solution with $\dot{p} \neq 0$.

For a given arch a numerical solution of the nonlinear boundary-value problem governed by equations (16) and (17) yields a point on the P versus v_c curve, but provides no information regarding the corresponding values of the stiffness coefficients C_{ij} . However, these coefficients can be calculated by solving differential equations which are derived from equations (16) and (17) and are linear in the rates. In a quasi-static deformation of the arch such that equations (16) and (17) are satisfied we may consider the dependent variables θ , x , and y to be functions of u_c , v_c , β_c , and w as well as functions of ϕ , and we may consider V_0 , H , R , P , and M_c to be functions of u_c , v_c , β_c , and w . Rate equations are derived by differentiating equations (16) and (17). Thus

$$\begin{aligned} \kappa^2 EJ\dot{\theta}'' + \dot{\theta}H \cos \theta - \dot{\theta}(V_0 - aw\phi) \sin \theta + \dot{H} \sin \theta \\ + (\dot{V}_0 - aw\phi) \cos \theta = 0 \end{aligned} \quad (20)$$

$$\dot{x}' = -a\dot{\theta} \sin \theta, \quad \dot{y}' = a\dot{\theta} \cos \theta \quad (21)$$

in which

$$\begin{aligned} \dot{\theta} &= \frac{\partial \theta}{\partial u_c} \dot{u}_c + \frac{\partial \theta}{\partial v_c} \dot{v}_c + \frac{\partial \theta}{\partial \beta_c} \dot{\beta}_c + \frac{\partial \theta}{\partial w} \dot{w} \\ \dot{x} &= \frac{\partial x}{\partial u_c} \dot{u}_c + \frac{\partial x}{\partial v_c} \dot{v}_c + \frac{\partial x}{\partial \beta_c} \dot{\beta}_c + \frac{\partial x}{\partial w} \dot{w} \\ \dot{y} &= \frac{\partial y}{\partial u_c} \dot{u}_c + \frac{\partial y}{\partial v_c} \dot{v}_c + \frac{\partial y}{\partial \beta_c} \dot{\beta}_c + \frac{\partial y}{\partial w} \dot{w} \\ \dot{V}_0 &= \frac{\partial V_0}{\partial u_c} \dot{u}_c + \frac{\partial V_0}{\partial v_c} \dot{v}_c + \frac{\partial V_0}{\partial \beta_c} \dot{\beta}_c + \frac{\partial V_0}{\partial w} \dot{w} \\ \dot{H} &= \frac{\partial H}{\partial u_c} \dot{u}_c + \frac{\partial H}{\partial v_c} \dot{v}_c + \frac{\partial H}{\partial \beta_c} \dot{\beta}_c + \frac{\partial H}{\partial w} \dot{w} \end{aligned} \quad (22)$$

and

$$\dot{\theta}'' = \frac{\partial^2 \dot{\theta}}{\partial \phi^2}, \quad \dot{x}' = \frac{\partial \dot{x}}{\partial \phi}, \quad \dot{y}' = \frac{\partial \dot{y}}{\partial \phi}$$

To these equations we append a rate formulation of the relation between moment and change of curvature,

$$\dot{M} = EJK\dot{\theta}' \quad (23)$$

and the boundary conditions at the supports,

$$\dot{x} = \dot{y} = \dot{\theta} = 0, \quad \dot{x}' = \dot{y}' = \dot{\theta}' = 0 \quad (24)$$

Finally, we include rate equations of equilibrium in terms of forces at the load point. Thus

$$\begin{aligned} \dot{R} &= \dot{H} - \dot{\bar{H}} \\ \dot{P} &= \dot{\bar{V}}_0 + \dot{V}_0 \\ \dot{M}_c &= \dot{\bar{M}}(0) - \dot{M}(0) \end{aligned} \quad (25)$$

In equations (24) and (25), a superposed bar indicates that the corresponding quantity is associated with the portion of the arch

² This statement, of course, amounts to a definition of what is meant by a limit point.

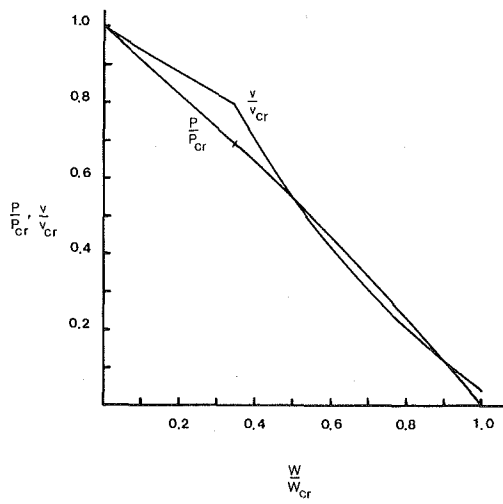


Fig. 1 P/P_{cr} versus w/w_{cr} for $\alpha = 30$ deg

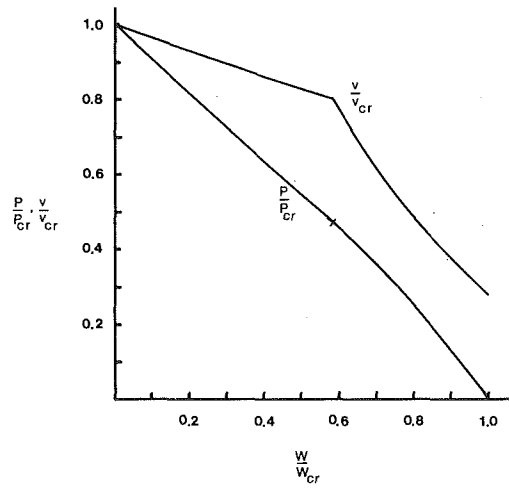


Fig. 2 P/P_{cr} versus w/w_{cr} for $\alpha = 80$ deg

between the load point and the left support. Unbarred quantities are associated with the segment of arch between the right support and the load point.

If an equilibrium configuration of the arch is known for given values of u_c , v_c , β_c , and w , then the solution of equations (20) and (21) and the boundary conditions, all of which are linear in the rates, for each half of the arch may be inserted in equations (25) to obtain the coefficients C_{ij} and b_i in equations (18). The rates $\dot{\theta}$, \dot{x} , and \dot{y} , are obtained from equations (22). It is observed that for sufficiently small increments in u_c , v_c , β_c , and w , equations (22) and (18) can be used in an obvious way to determine increments $\Delta\theta$, Δx , Δy , ΔR , ΔP , and ΔM_c such that the arch is in equilibrium under the incremented loads $R + \Delta R$, $P + \Delta P$, $M_c + \Delta M_c$, $w + \Delta w$ in the configuration $\theta + \Delta\theta$, $x + \Delta x$, $y + \Delta y$. Moreover, if the determinant of the C_{ij} is nonzero, the load increments may be specified and equations (18), written in terms of increments, may be solved to determine the required increments in u_c , v_c , β_c for equilibrium under the incremented loads. With knowledge of this new equilibrium state the process can be repeated to obtain another equilibrium state and by continuing in this way one can determine an entire load-deformation history for an arch. This then is the essence of the procedure used to generate the numerical results presented herein.

The procedure for the calculation of C_{i1} is typical of that used to calculate all of the C_{ij} and b_i . We set $\dot{u}_c = 1$, $\dot{v}_c = \dot{\beta}_c = \dot{w} = 0$, and, since continuity of $\dot{\theta}$, \dot{x} , and \dot{y} is required at the load point, we take

$$\begin{aligned}\dot{V}_0 &= \frac{\partial V_0}{\partial u_c}, \quad \dot{H} = \frac{\partial H}{\partial u_c}, \quad \dot{M}(0) = EJK \frac{\partial}{\partial \phi} \left(\frac{\partial \theta}{\partial u_c} \right)_{\phi=0} \\ \dot{V}_0 &= \frac{\partial \bar{V}_0}{\partial u_c}, \quad \dot{H} = \frac{\partial \bar{H}}{\partial u_c}, \quad \dot{M}(0) = EJK \frac{\partial}{\partial \bar{\phi}} \left(\frac{\partial \bar{\theta}}{\partial u_c} \right)_{\bar{\phi}=0}\end{aligned}$$

as six constants to be determined such that boundary conditions (24) will be satisfied. Equations (25) then yield the coefficients C_{i1} . The procedure for calculating the C_{ij} is seen to be essentially identical to the procedure employed to calculate stiffness coefficients in the small deflection theory of structures.

In the numerical work, central finite-difference equations were used in solving the rate equations, and a Runge-Kutta procedure was used to calculate the incremental changes in θ . An idea of the accuracy of the method can be obtained by considering the symmetric deformation of a weightless semicircular hinged arch subjected to a vertical downward point load at the crown for which the exact solution can be expressed in terms of elliptic integrals. For $v_c = 0.195a$ (a very large deflection that produces a change in sign of the curvature κ^* in the deformed state), the exact value of the load and the value determined by the numeri-

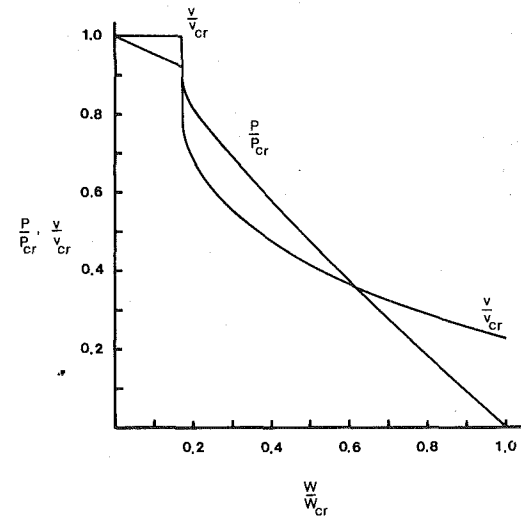


Fig. 3 P/P_{cr} versus w/w_{cr} for $\alpha = 130$ deg

cal method agree to within 0.03 percent. In the foregoing solution, as in the solutions presented herein, the arch was divided into 200 equal parts. In the case of the weightless arch considered above the increment in v_c was 0.005a. For own weight loading, the increments, Δv_c , used in obtaining the results presented herein were in the range 0.0008 to 0.004a. Expressed as a fraction of the deflection at buckling, v_{cr} , $\Delta v_c \approx 0.045v_{cr}$ for $\alpha = 30$ deg and $\Delta v_c < 0.028v_{cr}$ for all other values of α .

Calculated Results

The buckling behavior of circular arches with clamped ends is more complex than that of two-hinged arches. While a high-rise arch with hinged ends always buckles asymmetrically swaying to the side, the steep clamped arch can lose its stability either in a symmetric (snap-through) or an asymmetric (sideways) mode, depending on the relative magnitudes of the two loads. The asymmetric sideways buckling mode is characterized by a bifurcation point in the load-deflection diagrams, while the symmetric snap-through buckling mode is accompanied by a simple maximum in the load-deflection plot.

Typical critical load interaction curves for hingeless circular arches are plotted in Figs. 1-3³ for $\alpha = 30$, 80, and 130 deg. The

³ These figures also present crown deflection corresponding to the critical loads.

Table 1 Clamped arches

α	$w = 0$		$P = 0$		
	$P_{cr}a^2/EI$	v_{cr}/a	$w_{cr}a^3/EI$	$w_{cr}a^2/EI$	v_{cr}/a
30°	28.591	0.0450	74.77	78.30	0.001766
40°	21.610	0.08127	42.495	59.33	0.005498
50°	17.4674	0.1310	27.468	47.94	0.01425
60°	14.7496	0.1916	19.216	40.25	0.03121
70°	12.852	0.2688	14.132	34.53	0.05943
80°	11.475	0.3629	10.716	29.92	0.09966
90°	10.4522	0.4765	8.245	25.90	0.1463
100°	9.6933	0.6123	6.337	22.12	0.1904
110°	9.1355	0.7720	4.798	18.42	0.2246
120°	8.7471	0.9573	3.5665	14.94	0.2492
130°	8.5123	1.1686	2.6155	11.87	0.26695

Table 2 Points (values) at which the two modes of buckling coexist

α	P_i/P_{cr}	v_i/v_{cr}	w_i/w_{cr}
30°	0.692	0.795	0.345
40°	0.641	0.775	0.398
50°	0.587	0.753	0.452
60°	0.533	0.755	0.513
70°	0.487	0.768	0.558
80°	0.470	0.800	0.587
90°	0.488	0.845	0.593
100°	0.547	0.895	0.565
110°	0.635	0.945	0.505
120°	0.768	0.980	0.380
130°	0.920	0.999	0.172

left portions of the load interaction diagrams correspond to the symmetrical (snap-through) buckling mode. They are nearly straight (slightly concave away from the origin) for all hingeless arches investigated, $\alpha = 30, 40, \dots, 130$ deg, and can be approximated by a linear equation of the type

$$\frac{P}{P_{cr}} = 1 - \frac{w_{cr}}{w_i} \left(1 - \frac{P_i}{P_{cr}} \right) \frac{w}{w_{cr}}, \quad \frac{w}{w_{cr}} < \frac{w_i}{w_{cr}} \quad (26)$$

where w_i/w_{cr} , P_i/P_{cr} are the coordinates of the point of intersection of the interaction curves corresponding to snap-through and sidesway. The values of P_{cr} and w_{cr} are listed in Table 1 and those of w_i/w_{cr} and P_i/P_{cr} in Table 2 for different magnitudes of α .

The right portions of the interaction curves for the critical load P and weight w correspond to the asymmetrical buckling (sidesway) mode. As a rule, they are more curved than the left portions. However, for design purposes they also can be approximated by straight lines given by the equation

$$\frac{P}{P_{cr}} = \frac{P_i}{P_{cr}} \left(1 - \frac{w_i}{w_{cr}} \right)^{-1} \left(1 - \frac{w}{w_{cr}} \right), \quad \frac{w}{w_{cr}} > \frac{w_i}{w_{cr}} \quad (27)$$

which together with Table 1 will yield the critical values P of the concentrated load that are on the safe side (since this portion of the interaction curve is concave toward the origin) for arches with α = from 30 to 100 deg. The right-hand portion of the interaction curve for $\alpha = 110$ deg is nearly straight (it seems to have an inflection point) and can also be represented by the linear equation (27). For arches with $\alpha = 120$ and 130 deg these portions are

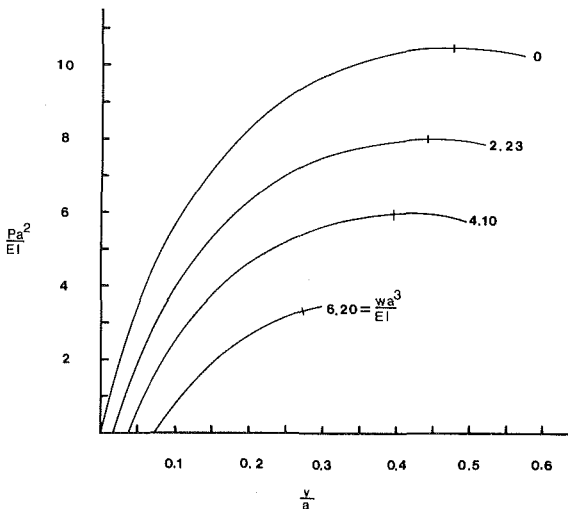
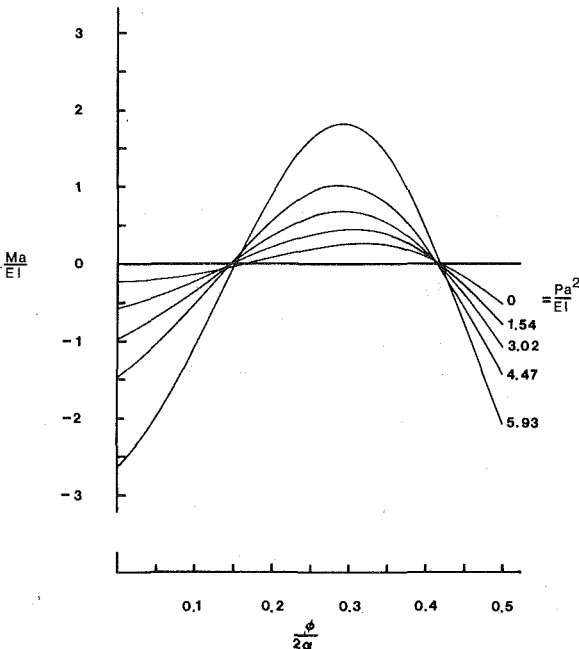


Fig. 4 Point load versus (prebuckling) crown deflection for heavy semi-circular arch

Fig. 5 Moment diagrams for the semicircular arch ($wa^3/EI = 4.10$)

convex toward the origin and not sufficiently straight for a straight-line approximation.

Figs. 1-3 also depict the variation of the downward crown displacement with the critical values of the loads at the instant of buckling. The intersections of the two v_c/v_{cr} versus w/w_{cr} curves are the points at which the two buckling modes can coexist. The coordinates of these intersection points are presented in Table 2 for arches with $\alpha = 30, 40, \dots, 130$ deg. Fig. 4 displays four plots of the point load P versus downward crown displacement v_c for four different weights of the semicircular arch (normal dashes indicate loss of stability). Figs. 5 and 6 present samples of moment and thrust diagrams for a heavy semicircular arch under load P not exceeding critical values.

Discussion and Conclusions

It has been found that hingeless elastic circular arches of uniform cross section subjected to a downward point load at the crown and their own weight can buckle either asymmetrically by

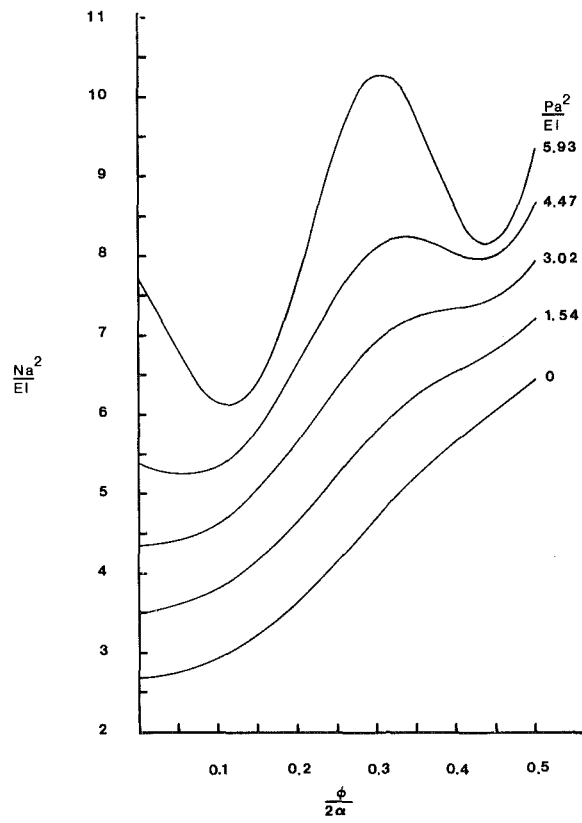


Fig. 6. Thrust diagrams for the semicircular arch ($wa^3/EI = 4.10$)

abrupt sidesway (a bifurcation type of buckling), if heavy, or symmetrically by snap-through, if light. These findings qualitatively do not contradict the results obtained for shallow arches with clamped ends in [15] on the basis of a rather accurate shallow-arch theory. Moreover, the conclusion reached in [15] that for clamped shallow arches under a concentrated load, asymmetrical buckling does not occur until after the first maximum load has been reached and therefore the symmetrical buckling criterion governs this problem, applies as well to nonshallow circular arches with $\alpha \leq \alpha^* \approx 135$ deg [7].⁴

When an arch is said to buckle by symmetric snap-through, this does not mean absence of bifurcation points in the calculated load-deflection curves and surfaces; it simply means that symmetric loss of stability takes place prior to sidesway in the case of an unconstrained arch with hingeless supports.

A comparison of the results obtained herein for hingeless arches with the solutions presented in [13, 16] for two-hinged arches demonstrates that, for the loads considered, hingeless circular arches may buckle by either asymmetrical sidesway or symmetrical snap-through, depending on the relative magnitudes of the point load and the weight of the arch, while two-hinged nonshallow circular arches buckle only asymmetrically by sidesway.

The plots of the interaction curves of the critical values of the point load and the weight indicate that, for practical arch dimensions, these curves may be approximated by two segments of

⁴The effect of weight on large deflections of shallow clamped arches is discussed in [17].

straight lines, a fact of importance to the designer. With the aid of the interaction plots, or the simple linear formulas and two tables, the experimenter will be able to compare his test results determined on heavy arches with the theoretical values for arches under the point load acting singly. For example, for an arch with $\alpha = 45$ deg, $P_{cr} = 19.30 EI/a^2$, $w_{cr} = 33.7 EI/a^3$ (see [7, 6]) and $P_i/P_{cr} \approx 0.614$, $w_i/w_{cr} \approx 0.425$ from Table 2. Equation (26) yields then $Pa^2/EI \approx 19.3 (1 - 0.027 wa^3/EI)$. For the steel arches considered in [8], $wa^3/EI = 0.347$ and with the correction for the effect of own weight the calculated buckling load becomes $P = 19.1EI/a^2$. The experimental values in [8] are now determined to be 3.1 and 6.3 percent less than the calculated buckling load. It is observed that for the arches in [8], the effect of own weight is to reduce the calculated critical point load by about 1 percent.

Acknowledgment

This investigation was supported by the National Science Foundation Grant GK-19726.

References

- 1 Huddleston, J. V., "Finite Deflections and Snap-Through of High Circular Arches," *JOURNAL OF APPLIED MECHANICS*, Vol. 35, No. 4 TRANS. ASME, Vol. 90, Series E, Dec. 1968, pp. 763-769.
- 2 DaDeppo, D. A., and Schmidt, R., "Sidesway Buckling of Deep Circular Arches Under a Concentrated Load," *JOURNAL OF APPLIED MECHANICS*, Vol. 36, No. 2, TRANS. ASME, Vol. 91, Series E, June 1969, pp. 325-327.
- 3 Langhaar, H. L., Boresi, A. P., and Carver, D. R., "Energy Theory of Buckling of Circular Elastic Rings and Arches," *Proceedings of Second U.S. National Congress of Applied Mechanics*, June 1954, pp. 437-443.
- 4 Lind, N. C., "Elastic Buckling of Symmetrical Arches," University of Illinois Engineering Experiment Station Technical Report No. 3, 1962.
- 5 DaDeppo, D. A., and Schmidt, R., "Nonlinear Analysis of Buckling and Postbuckling Behavior of Circular Arches," *Zeitschrift für angewandte Mathematik und Physik*, Vol. 20, No. 6, 1969, pp. 847-857.
- 6 Schmidt, R., and DaDeppo, D. A., "Critical Weights and Deflections of Clamped, Heavy, Circular Arches," *Journal of the Franklin Institute*, Vol. 293, No. 5, May 1972, pp. 371-374.
- 7 Schmidt, R., and DaDeppo, D. A., "Buckling of Clamped Circular Arches Subjected to a Point Load," *Zeitschrift für angewandte Mathematik und Physik*, Vol. 23, 1972, pp. 146-148.
- 8 Nordgren, R. P., "On Finite Deflection of an Extensible Circular Ring Segment," *International Journal of Solids and Structures*, Vol. 2, No. 2, Apr. 1966, pp. 223-233.
- 9 DaDeppo, D. A., and Schmidt, R., "Stability of Heavy Circular Arches with Hinged Ends," *AIAA Journal*, Vol. 9, No. 6, June 1971, pp. 1200-1201.
- 10 Schmidt, R., and DaDeppo, D. A., "Large Deflections of Eccentrically Loaded Arches," *Zeitschrift für angewandte Mathematik und Physik*, Vol. 21, No. 6, 1970, pp. 991-1004.
- 11 Patrick, G. E., Jr., "Numerical Methods for the Nonlinear Analysis of an Elastic Arch," Report No. RS-TR-68-15, U.S. Army Missile Command, Redstone Arsenal, Ala., Dec. 1968.
- 12 Sharifi, P., and Popov, E. P., "Nonlinear Buckling Analysis of Sandwich Arches," *Journal of the Engineering Mechanics Division, Proceedings, ASCE*, Vol. 97, No. EM5, Oct. 1971, pp. 1397-1412.
- 13 DaDeppo, D. A., and Schmidt, R., "Stability of Two-Hinged Circular Arches With Independent Loading Parameters," *AIAA Journal*, Vol. 12, No. 3, Mar. 1974, pp. 385-386.
- 14 Schmidt, R., and DaDeppo, D. A., "A Survey of Literature on Large Deflections of Nonshallow Arches. Bibliography of Finite Deflections of Straight and Curved Beams, Rings, and Shallow Arches," *Industrial Mathematics, The Journal of the IMS*, Vol. 21, Part 2, 1971, pp. 91-114.
- 15 Schreyer, H. L., and Maser, E. F., "Buckling of Shallow Arches," *Journal of the Engineering Mechanics Division, Proceedings, ASCE*, Vol. 92, No. EM4, Aug. 1966, pp. 1-19.
- 16 DaDeppo, D. A., and Schmidt, R., "Stability of an Arch Under Combined Loads; Bibliography on Stability of Arches," *Industrial Mathematics*, Vol. 20, Part 2, 1970, pp. 71-89.
- 17 Kennedy, J. S. and Aggarwal, A. S., "Effect of Weight on Large Deflections of Arches," *Journal of the Engineering Mechanics Division, Proceedings, ASCE*, Vol. 97, No. EM3, June 1971, pp. 637-644.